Angle-resolved photoemission spectroscopy study of Te-annealed superconducting FeTe$_{1-x}$Se$_x$

Keisuke KOSHIISHI[1,*], Takumi OTSUKA[2], Chun LIN[1], Masahiro SUZUKI[1], Yuxuan WAN[1],

Hiroshi KUMIGASHIRA[3], Koji HORIBA[3], Takao WATANABE[2] and Atsushi FUJIMORI[1]

[1] Department of Physics, University of Tokyo, 7-3-1 Hongo, Bunkyo-ku, Tokyo, 113-0033, Japan

[2] Graduate School of Science and Technology, Hirosaki University, 3, Bunkyo-cho, Hirosaki-shi, Aomori-ken, 036-8561, Japan

[3] Photon Factory, High Energy Accelerator Research Organization, 1-1 Oho, Tsukuba, Ibaraki, 305-0801, Japan

1 Introduction

11-type iron-based superconductors have the simplest crystal structure in which layers consisting of Fe atoms tetrahedrally coordinated by chalcogens (e.g. Te, Se) stack. The parent compound FeTe shows a bi-collinear double-stripe antiferromagnetic (AFM) order with the wave vector Q=($\pi/2$, $\pi/2$), which is distinct from the usual collinear magnetic structure observed in other parent compounds like BaFe$_2$As$_2$ [1]. As tellurium in the parent compound is gradually replaced by selenium, the AFM order is suppressed and superconductivity is observed. It has been reported that the superconductivity is affected by excess Fe located at interstitial sites and very sensitive to its stoichiometry. By annealing a specimen, the excess Fe can be removed, and then the superconductivity can be improved [2,3]. The superconductivity with the superconducting transition temperature (T_c) of ~10 K is observed in the wide low Se-concentration region from x = 0.05 up to 0.5 and the maximum bulk T_c reaches 14.5 K at x ~ 0.4. According to a recent transport measurement for Te-annealed samples [4], although the Hall coefficient (R_H) of annealed FeTe$_{0.6}$Se$_{0.4}$ is almost independent of temperature above 50 K, it decreases with decreasing temperature below 50 K and eventually changes their sign from positive to negative around 30 K, indicating multi-carrier features of holes and electrons in optimally doped samples. Moreover, the strong temperature dependence with the sign change suggests that band-specific pseudo gaps may open. On the other hand, for FeTe$_{0.8}$Se$_{0.2}$, R_H is always positive similar to the case of as-grown samples. Naively, this behavior indicates that contribution to the transport properties dominantly comes from hole carriers in contrast to the optimally doped sample. However, since Fe-based superconductor has multi-orbital nature because the $3d$ states of Fe form bands near the Fermi level, it is not clear whether such simple scenario is valid or not. Therefore, we have performed angle-resolved photoemission spectroscopy (ARPES) measurements on FeTe$_{1-x}$Se$_x$ in order to investigate differences in the electronic structure between the optimally doped and low Se-doped samples and the temperature dependence of their electronic structures.

2 Experiment

High-quality single crystals of FeTe$_{1-x}$Se$_x$ were grown using the Bridgman method and annealed in a tellurium vapor ("Te-anneal"). To check the T_c, magnetization measurements were carried out by using a Magnetic Property Measurement System-5S (Quantum Design, Co., Ltd.) at The University of Tokyo Cryogenic Research Center. ARPES measurements were performed at beamline 28A of Photon Factory using circularly polarized light with the photon energy of 54 eV corresponding to $k_z \approx 0$. A SIENTA SES-2002 electron analyzer was used with the total energy resolution of ~ 20 meV. The crystals were cleaved *in situ* below T = 20 K, and the measurements were carried out in an ultrahigh vacuum of ~ 9×10^{-11} Torr.
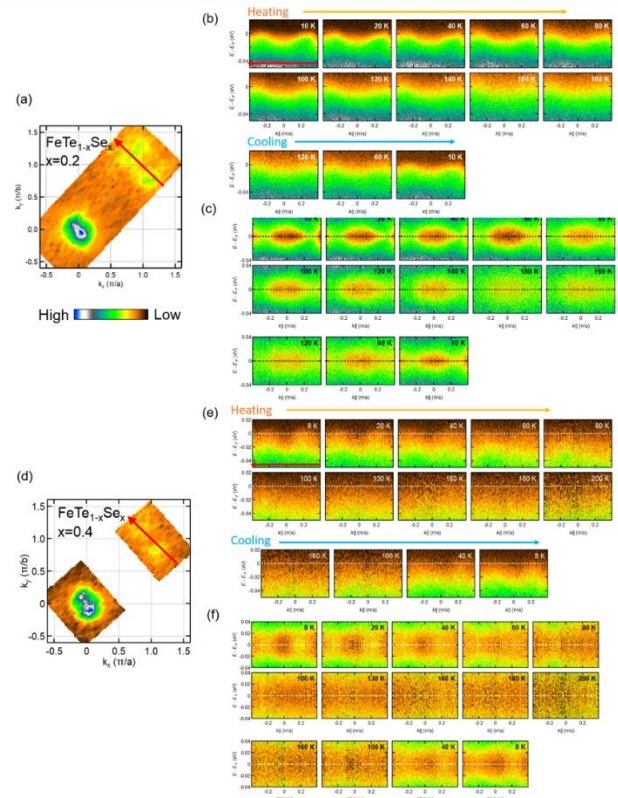
Fig. 1: Temperature evolution of the electron bands around the zone corner of Te-annealed FeTe$_{1-x}$Se$_x$ (x=0.2 and 0.4). (a) In-plane Fermi surface of x=0.2. (b), (c) Temperature evolution of the energy-momentum plots around the M point and those symmetrized with respects to the Fermi level to highlight Fermi momentum positions, respectively. (d), (e), (f) The same as (a), (b) and (c) for x=0.4,

respectively. Cuts are along red arrows in (a) and (d).

3 Results and Discussion

Figure 1 shows the temperature evolution of the electron band around the zone corner of Te-annealed $FeTe_{1-x}Se_x$ (x=0.2 and 0.4) from 10 K up to 200 K. The cuts are along the red arrows in Figs. 1(a) and 1(d). Intensity plots are shown in Figs. 1(b) and 1(e). One can see that the electron band is broadened and becomes indistinct with increasing temperature due to temperature broadening. To highlight the k_F positions, the ARPES spectra symmetrized along the energy direction with respects to E_F are shown in Figs. 1(c) and 1(f). Interestingly, in the case of x=0.2, distance between the different k_F's seems to expand with increasing temperature, suggesting the expansion of the electron pocket. For x=0.4, as temperature increases, spectral intensity is weakened and eventually disappears. One may suspect the possibility of electron doping or impurity scattering on the sample surface due to contamination of the sample surface. However, in our measurements, we have also measured ARPES spectra with cooling from the highest temperature (180 K for x=0,2 and 200 K for x=0.4) to the lowest temperature (10 K for x=0.2 and 8 K for x=0.4) after heating, and similar spectra were obtained at the lowest temperature. This reproducibility proves that the temperature evolution of the observed spectra is intrinsic.
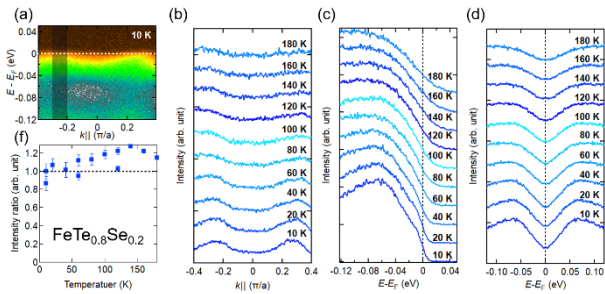
Fig. 2: Temperature evolution of the spectra of the electron band in Te-annealed $FeTe_{0.8}Se_{0.2}$. (a) ARPES spectra at 10 K. (b) Temperature evolution of the momentum distribution curve (MDC) integrated within $E_F \pm 10$ meV from 10 K up to 180 K. (c) Temperature evolution of the energy distribution curve (EDC) obtained by integrating MDCs within momentum region of $k_F \pm 0.05\pi/a$ indicated by shaded section in (a). (d) Symmetrized EDCs shown in (c) with respects to E_F. (f) Temperature dependence of spectral weight around E_F. The intensity has been by integrating the symmetrized EDCs within the energy range of $E_F \pm 10$ meV, and normalized to that at the lowest temperature (10 K).

For more detailed analysis, we have plotted the momentum distribution curve (MDCs) and EDCs at different temperatures in Figs. 2 and 3. As has been pointed out above, for x=0.2, an MDC-peak shift with temperature can be recognized (Fig. 2(b)). In Fig. 2(c), a small shoulder structure around -10 meV arising from the electron band near E_F was observed at 10 K, and it is attenuated at high temperatures due to the temperature broadening. For x=0.4, although MDC and EDC peaks can be recognized in the

low temperature region, both intensities were too weak to examine peak positions above 100 K. Their trends are similar to each other. Namely, as temperature increases, the peak structure is obscured. EDCs that have been symmetrized in order to eliminate the temperature broadening are also shown in Figs. 2(d) and 3(d).
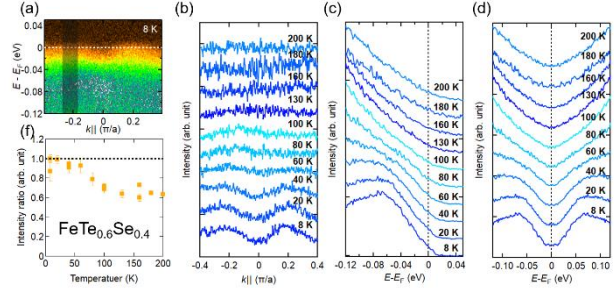
Fig. 3: Temperature evolution of the spectra of the electron band in Te-annealed optimally-doped $FeTe_{0.6}Se_{0.4}$. (a) ARPES spectra at 8 K. (b) Temperature evolution of the MDC integrated within $E_F \pm 10$ meV from 8 K up to 200 K. (c) Temperature evolution of the EDC obtained by integrating MDCs within momentum region of $k_F \pm 0.05\pi/a$ indicated by shaded section in (a). (d) Symmetrized EDCs shown in (c) with respects to E_F. (f) Temperature dependence of spectral weight around E_F. The intensity ratio has been obtained by integrating the symmetrized EDCs within the energy range of $E_F \pm 10$ meV, and normalized to that at the lowest temperature (8 K).

For quantitative comparison of the density of states (DOS) near E_F, in Figs. 2(f) and 3(f), we have plotted intensities near E_F obtained by integrating symmetrized EDC within the energy range of $E_F \pm 10$ meV as a function of temperature. They have been normalized to the intensity at the lowest temperature (10 K for x=0.2 and 8 K for x=0.4). In the case of the Se-underdoped sample, the intensity near the Fermi level is nearly constant or grows slightly with heating, indicating the insensitivity of the DOS near E_F to temperature. On the other hand, the intensity near E_F of the optimally-doped =0.4 sample depends on temperature in a characteristic way (Fig. 3(f)). The intensity decreases with increasing temperature in the temperature region below 100 K although it is independent of temperature above l30 K, which suggests that the DOS of the electron band around the zone corner decreases with increasing temperature, indicating the suppression of the coherent peak of the electron band and the disappearance of the electron pocket, in contrast to Se-underdoped compound. Therefore, we consider that spectral weight is transferred from the coherent states to incoherent states with temperature, similar to the case of the d_{xy} band around Γ [5]. According to the magneto-transport measurements, the Hall coefficient of the optimally-doped compound also depends on temperature only blow ~150 K and increases with heating in the temperature region below ~75 K, similar to the temperature dependence of the coherent peak of the electron band in the optimally doped compound. For the relationship between the Hall coefficient and the electronic states, we have depicted schematic pictures for

the Fermi surfaces predicted by present results in Fig. 4. In the low Se-doped compound, the electron band does not exhibit drastic changes within the temperature range below 200 K except for the slight k_F shift. If the hole surfaces also do not change, the Fermi surfaces should not change. In that case, one cannot attribute the temperature dependence of the Hall coefficient to the evolution of the Fermi surface. One possibility is that antiferromagnetic fluctuation corresponding to the antiferromagnetic order observed in the parent compound FeTe affects charge carriers in compounds close to the parent compound. In the case of cuprates [6], it has been theoretically suggested that antiferromagnetic fluctuations can give rise non-trivial temperature dependence of the Hall coefficient, which differs from the prediction from the Fermi surface topology. On the other hand, for the optimally-doped compound, we could not observed the electron band at high temperatures, indicating the disappearance of the electron pocket. Assuming that the hole bands in the Te-annealed sample exhibit the temperature dependence similar to as-grown samples [5], the optimally doped compound would have only a small hole pocket centered at Γ. Taking into account the charge carrier concentration estimated from the enclosed area of the Fermi surface at low temperature, the charge carrier concentration is 0.03 holes/unit cell in $x=0.4$ in the high temperature region, which is comparable to that of $x=0.2$. The similar carrier concentrations may cause similar magnitudes of Hall coefficient between them at high temperature. In order to completely clarify the temperature evolution of the electronic states of Te-annealed $FeTe_{1-x}Se_x$, the hole bands at high temperatures remain to be studied systematically.

the optimally-doped compound in contrast to its temperature independent behavior for the Se-underdoped compound, indicating the disappearance of the electron pockets. Moreover, the possible changes of the Fermi surface topology predicted from the present results explain the temperature dependence of the Hall coefficient. However, since we have clarified only the temperature dependence of the electron band and the hole bands at high temperature is still uncertain, further work is necessary in order to fully clarify the temperature evolution of the electronic states in Te-annealed $FeTe1-xSex$.

References
[1] S. Li *et al*., Phys. Rev. B **79**, 054503 (2009).
[2] Y. Sun *et al*., Sci. Rep. **6**, 32290 (2016)
[3] Y. Koshika *et al*., J. Phys. Soc. Jpn. **82**, 023703 (2013)
[4] T. Otsuka *et al*., Phys. Rev. B **99**, 184505 (2019)
[5] M. Yi *et al*., Nat. Commun. **6**, 7777 (2015).
[6] H. Kontani, Reports Prog. Phys. **71**, 026501 (2008)

* keisuke@wyvern.phys.u-tokyo.ac.jp
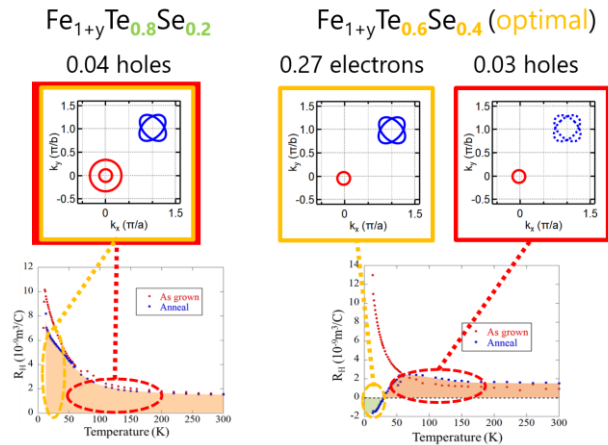
Fig. 4: Schematic picture of the temperature evolution of the Fermi surface in Te-annealed $FeTe_{1-x}Se_x$.

In conclusion, in order to clarify the temperature evolution of the band structure and the relationship between the Hall coefficient and the electronic structure, in $FeTe_{1-x}Se_x$, in which the excess Fe atoms are completely removed, we have carried out ARPES measurements of Te-annealed FeTe1-xSex ($x=0.2$ and 0.4). Upon increasing temperature, the coherent peak of the electron band around the zone corner weakens and disappears above 100 K in